

Environmental influence on structural health monitoring systems

J.-H. Bartels

Institute of Concrete Structures, TU Dresden, Dresden, Germany

M. Kitahara

Department of Civil Engineering, The University of Tokyo, Tokyo, Japan

S. Marx

Institute of Concrete Structures, TU Dresden, Dresden, Germany

M. Beer

Institute for Risk and Reliability, Leibniz University Hannover, Hannover, Germany

Institute for Risk and Uncertainty, University of Liverpool, Liverpool, UK

ABSTRACT: Monitoring is becoming increasingly important for the condition assessment of structures, as it allows continuous assessment. The aim is to identify changes in the condition of the structure that cannot be detected by purely visual inspection. In this paper, a typical measurement system used in practice is investigated under laboratory conditions with regard to its temperature dependence. A method for temperature compensation of laser distance measurements is presented and a Bayesian model updating is applied, with which a temperature compensation function over time can be determined semi-automatically. It is shown that the temperature-dependent transfer function should first be generated at the structure in order to perform a reliable temperature compensation. Furthermore, the application of Bayesian Model Updating shows a reliable fit of the temperature-dependent transfer function over time, so that the engineer is provided with a helpful tool for semi-automated temperature compensation in the case of time-variant behavior.

1 INTRODUCTION

For condition monitoring of structures, Structural Health Monitoring (SHM) is becoming increasingly important, as it allows continuous condition assessment of the structure and usefully supplements on-site inspections (Farrar and Worden 2007; Wedel and Marx 2022). The aim of monitoring is to identify changes in the condition of the structure that can only be inadequately detected by the purely visual inspection (Worden et al. 2007), whereby the goal of monitoring can only be achieved by comparing at least two different states: the reference state with the current state (Worden and Tomlinson 2019). For large infrastructures (e.g. wind turbines or bridges), however, the change in condition due to aging is very small (Hübler et al. 2022), so that precise measurements are required to be able to make reliable comparisons. The problem is that not only the behavior of the structure, but also other influences such as temperature affect the measurement signal. The question arises how such influences can be quantified and compensated.

This paper aims to make a contribution to this by investigating a measurement system typically used in practice under laboratory conditions with regard to its temperature dependence and its time-dependent behavior. For this, a method for temperature compensation is presented and Bayesian Model Updating (BMU) is applied, with which a temperature compensation function can be determined semi-automatically. This paper consists of five chapters. In

chapter 2, the measurement principle of the investigated Laser Triangulation Sensor (LTS) is explained and the principle of BMU is described. In chapter 3 the experimental setup with the measurement system used and the exposures are explained. On this basis, the temperature dependence of the measurement signal is analyzed. With the help of time-variant investigations, BMU is applied in chapter 4 and it is shown that a reliable updating of the temperature dependence over time is possible. Chapter 5 concludes with a summary and an outlook.

2 THEORIES AND METHODOLOGIES

2.1 Laser triangulation sensor – measurement principle

In this paper, LTS is used because it enables to investigate a simple measurement principle and it can be used in Offshore Wind Turbine (OWT) or bridge monitoring. The LTS measures the distance to an object surface by calculating the angle and provides a non-contact method of position measurement (Murakami 1994).

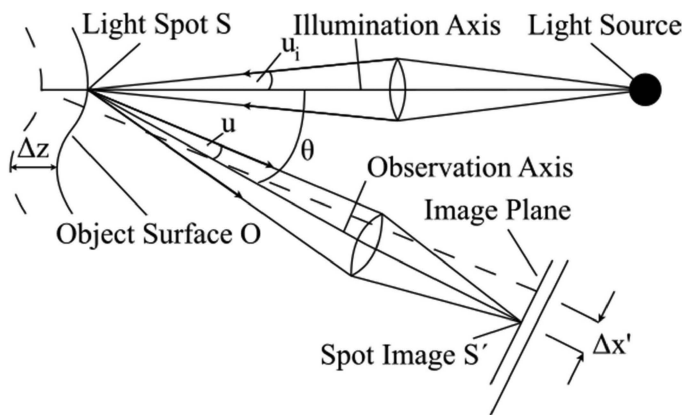


Figure 1. Measurement principle of LTS.

A laser beam is projected on the object surface O and a light spot S can be observed on it. The light spot is imaged through a lens with a numerical aperture $\sin(u_i)$ (Dorsch et al. 1994; Berns et al. 2019). The position of the spot image S' is determined with a position sensitive detector called photodiode array (PDA). The PDA is based on the CCD principle (charge-coupled device) and contains light sensitive electronic components using the internal photoelectric effect. From the position of the light spot on the image plane, the position of the measuring object is calculated (Löffler-Mang 2012). For a detailed description of the measurement principle, the reader is referred to Bartels et al. 2023.

2.2 Bayesian model updating – Transitional Markov Chain Monte Carlo (TMCMC)

For engineering problems, mathematical models are typically used to simulate and evaluate the behavior of structures under load conditions. This virtual behavior corresponds only poorly to the real physical structure. To solve this problem, model updating techniques can be applied to update physical input parameters. The parameters then describe e. g. material properties of a structure (Worden and Tomlinson 2019). These parameters are measured on the real structure and are integrated into the mathematical model of the virtual system to be updated, so that the difference between the mathematical model and the real physical behavior of the system is minimized.

The physical behavior of a system is described by a mathematical function $M(x; \vartheta)$, where x defines the vector of unchangeable model parameters and ϑ the vector of changeable model parameters to be updated. The mathematical relationship between the requested quantity

\mathbf{D} (e. g., the output of the measured distance by the LTS) and the mathematical prediction model $M(x; \vartheta)$ is defined by

$$\mathbf{D} = M(x; \vartheta) + \epsilon, \quad (1)$$

where ϵ describes the model or measurement error. The uncertainty in the model parameters ϑ can be accounted for using a probability density function (PDF). These problems are called forward problems because they can be solved analytically or with simple Monte Carlo simulations (Li and Caracoglia 2019). Monte Carlo simulation is used to generate the requested data \mathbf{D} for a known common PDF. The problem in reality is that the best-fit joint PDF is not known, which links the model parameters ϑ to the requested quantity \mathbf{D} . This is called the inverse problem (Lye et al. 2021). The advantage of implementing Bayesian inference in BMU process is that prior information about the requested model parameters ϑ can be combined with the observed data \mathbf{D} . Hence, the stochastic character of the quantity \mathbf{D} to be inferred can be generated. So, if a set of n independent and identically distributed observations ($D_1; D_2; \dots; D_n$) is made, then the pre-information is updated using Bayes' theorem (Mares et al. 2006). This leads to a posterior distribution of the requested model parameters ϑ under the condition of the observations made \mathbf{D}

$$P(\vartheta|\mathbf{D}) = \frac{P(\mathbf{D}|\vartheta) \cdot P(\vartheta)}{P(\mathbf{D})}, \quad (2)$$

where \mathbf{D} represents the observation vector, $P(\vartheta)$ the statistical distribution of the prior, $P(\mathbf{D}|\vartheta)$ the likelihood function, $P(\mathbf{D})$ the evidence, and $P(\vartheta|\mathbf{D})$ the posterior distribution. Instead of the analytical solution, the Monte Carlo method, which is easy to apply, is usually used. To apply the method, samples must be generated, which are performed using the iterative TMCMC sampler. For more detailed information on the TMCMC algorithm, please refer to Ching and Chen 2007.

3 EXPERIMENTAL SETUP AND TRANSFER FUNCTION

For the investigation of the temperature influence on laser measurements, a total of six LTSs within a measuring system is exposed to different temperatures within a climate chamber and analyzed whether and in which way the measurement signal changes.

3.1 Sensors, measurement system and environmental influence

The experimental setup is shown in Figure 2.

The entire measuring system consists of LTS, cable and measuring amplifier. As can be seen in Figure 2, the LTSs are fixed on a base plate with upstand and measure the horizontal distance to the upstand. The special feature: the base plate and the upstand are made of the material Alloy 36, an iron-nickel alloy with a small coefficient of thermal expansion of $\alpha_{T, \text{Alloy36}} = 0.50 \cdot 10^{-6} \text{ 1/K}$. Compared to this material, construction steel ($\alpha_{T, \text{Stahl}} = 13.00 \cdot 10^{-6} \text{ 1/K}$) has a coefficient of thermal expansion more than 20 times higher. With this design, it is possible to attribute changes in the measurement signal to the measurement system, since the influence of base plate strain due to temperature change is negligible. LTSs with a measuring range of 10 mm are tested, which measure within the measuring distances 16 mm to 26 mm. To examine the entire measurement range of the LTS, three initial distances d_{sel} between the sensor and the upstand are selected ($d_{\text{sel}} \approx [17 \text{ mm}; 21 \text{ mm}; 25 \text{ mm}]$).

3.2 Temperature-dependent transfer function

In the climate chamber, temperatures are varied between -10 °C and +50 °C in 10 K steps. The planned temperature curve can be seen in Figure 3.

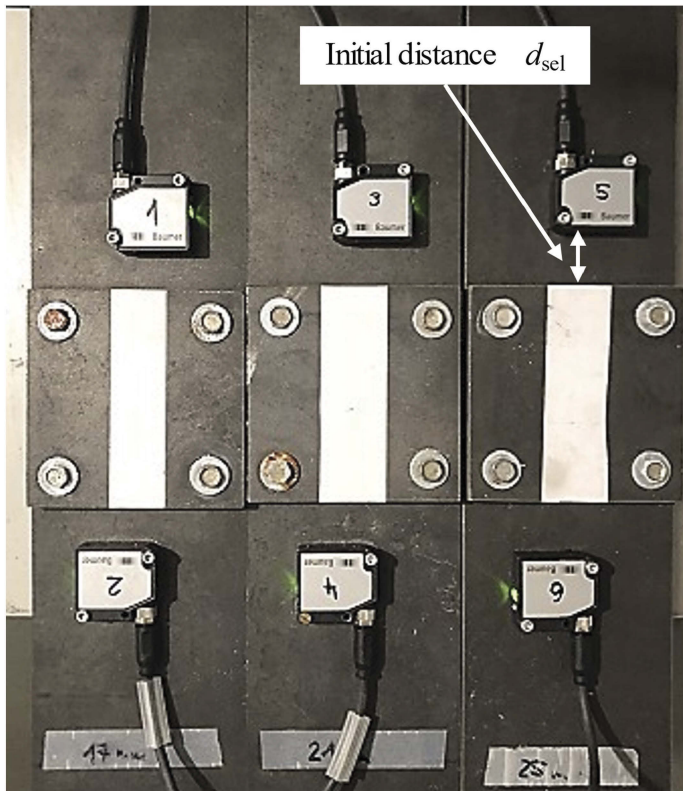


Figure 2. Experimental setup for the LTS investigation of temperature and time dependence.

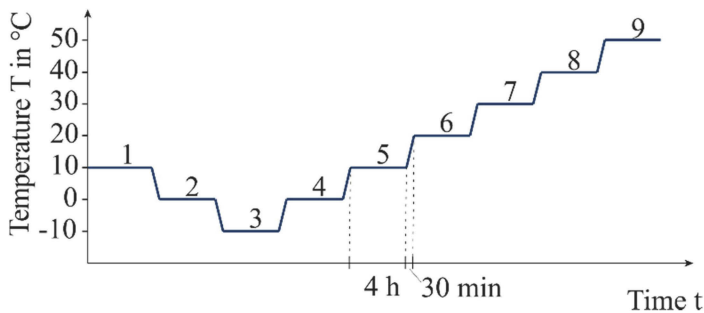


Figure 3. Intended temperature regulation for the determination of the temperature-dependent transfer function.

By varying the temperature, a reproducible test of the LTS with respect to the temperature dependence is possible. Each temperature level is kept constant for 4 h and the respective temperature change by 10 K is achieved within 30 min. Keeping the temperature constant for 4 h has two objectives: on the one hand, the temperature inertia of the experimental setup is overcome, so that the temperature can be assumed for the measuring system, the base plate and the ambient temperature. On the other hand, a representative amount of data can be generated over this period. With a sampling rate of 1 Hz, 14,400 measured values are generated over 4 hours. Only the constant temperature and measurement distance ranges are cut and the arithmetic mean is calculated as the expected value.

This procedure is carried out for all temperature levels, so that a total of seven expected values are calculated from -10 °C to +50 °C in 10 K steps. The values are related to the measured

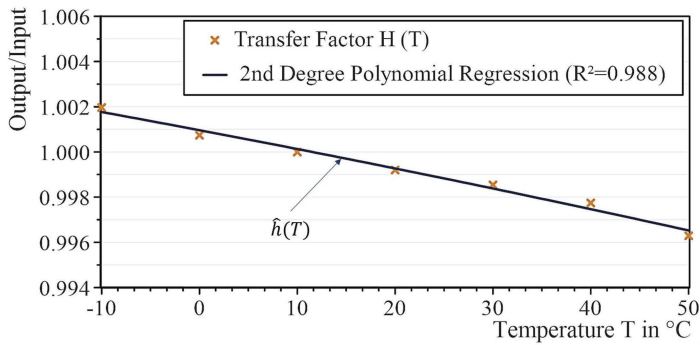


Figure 4. Temperature dependent transfer function for one LTS.

distance at 10 °C (reference value). This quotient between the measurement distance at a given temperature and the measurement distance at 10 °C is referred to as the transfer factor $H(T)$. The individual transfer factors are approximated by a 2nd degree regression polynomial to the so-called temperature-dependent transfer function (see Figure 4). The detailed description of the procedure for calculating the temperature-dependent transfer function is given in Bartels et al. 2022.

3.3 Time-dependence of the transfer function

With the knowledge of the temperature dependence of the LTS, the time dependence of the transfer function is to be analyzed in the next step. For this, the measurement system is subjected to a modified temperature and humidity curve (see Figure 5) using the same experimental setup as shown in Figure 2.

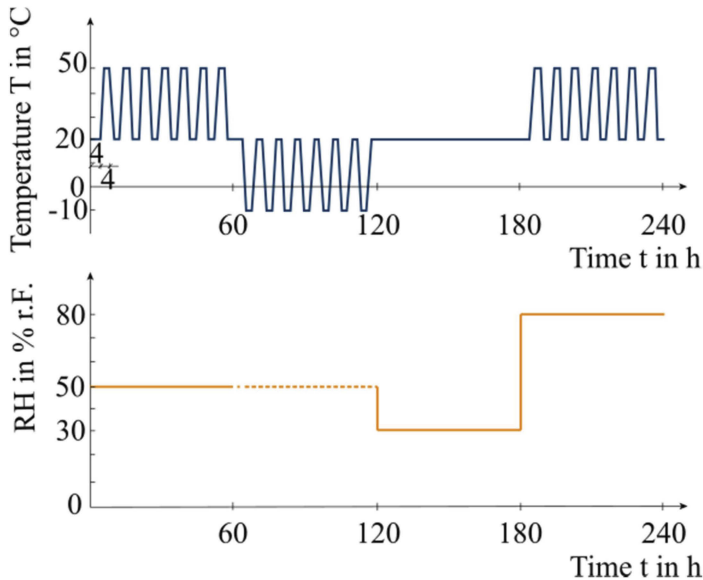


Figure 5. Intended temperature and humidity regulation for the aging tests.

The temperature and humidity can be divided into four phases, with each phase starting and ending at a temperature of 20 °C. This has the advantage that the measurement signal can be compared with the output signal (also at 20 °C) after each aging phase. In order to be able to record the time variance of the transfer function, the test for determining the temperature-dependent transfer

function according to chapter 3.2 is carried out after each 240-hour aging test and compared with the transfer function from Figure 4. The result is shown in Figure 6.

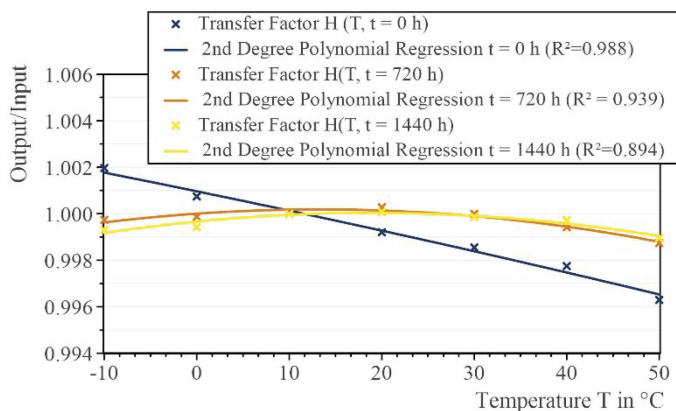


Figure 6. Investigation of the time variance of the temperature-dependent transfer function.

To enable the humidity to be controlled as well, the experimental setup had to be installed in a different climate chamber that can vary both the temperature and the humidity. At time $t = 0$ h the experimental setup is in the “old” climate chamber, at time $t = 720$ h the experimental setup is in the “new” climate chamber.

It can be clearly seen that the reconstruction of the measuring system has led to a change in the temperature-dependent transfer function. This circumstance means that this transfer function should only be determined in practice after successful installation of the measurement system on the structure when the system is no longer moved. A determination in the laboratory would lead to unreliable and non-reproducible results. After reconstruction the temperature-dependent transfer function does not change much over the considered test period of 1440 h, so that a time-invariant temperature-dependent transfer function can be assumed.

4 BAYESIAN MODEL UPDATING OF TRANSFER FUNCTION

The question arises whether the results from sections 3.2 and 3.3 can also be approximated with BMU. This would mean a partial automation of the measurement data evaluation and accordingly support the interpreting engineer in the quasi-real-time evaluation of the monitoring data. For this, the transfer function from the manual approximation is compared with the one generated by BMU. The result of the BMU is shown in Figure 7.

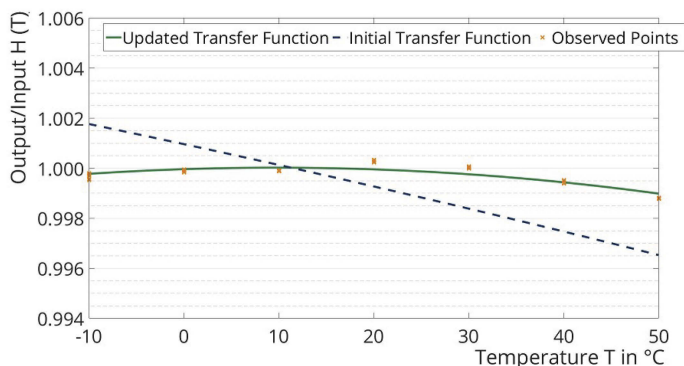


Figure 7. Transfer function calculated with BMU.

The initial transfer function at time point $t = 0$ h is updated for time point $t = 720$ h. The visual comparison between Figure 6 and Figure 7 shows a good agreement of the transfer functions at time point $t = 720$ h. This finding is quantified in the next step. For this, the mathematical model of the transfer function is important, which includes the parameters ϑ_i to be updated. With equation (3)

$$\hat{h}(T, \vartheta_i) = 1.00096 \cdot \vartheta_1 + (-8.18380 \cdot 10^{-5}) \cdot T \cdot \vartheta_2 + (-1.37294 \cdot 10^{-7}) \cdot T \cdot \vartheta_3 \quad (3)$$

the transfer function for updating is defined at time $t = 0$ h, where T describes the temperature. In the manual approximation of the transfer function at time $t = 720$ h, the parameters of the 2nd degree regression polynomial are determined so that they can be compared with the parameters of the transfer function at time $t = 0$ h. The quotient of the respective parameters results in the fitting factor ϑ_i . For the validation of BMU, the change of the transfer function is considered once between the time points $t = 0$ h to $t = 720$ h and between $t = 960$ h to $t = 1200$ h. The results are listed in Table 1.

Table 1. Comparison of manual approximation vs. BMU (TMCMC).

		ϑ_1	ϑ_2	ϑ_3
t = 0 h to 720 h	2 nd degree polynomial	0.99903	-0.33468	7.52741
	BMU (TMCMC)	0.99901	-0.35000	7.90000
	Error	0.002 %	4.576 %	4.950 %
t = 960 h to 1200 h	2 nd degree polynomial	1.00034	0.60755	0.68738
	BMU (TMCMC)	1.00025	0.65980	0.68000
	Error	0.008 %	8.600 %	1.074 %

It becomes clear that the error between manual approximation and BMU is small. Both in the updating process between strongly varying transfer functions ($t = 0$ h to 720 h) and in the case of similar transfer functions ($t = 960$ h to 1200 h), the procedure is accurate. Nevertheless, the fitting factors in the BMU process are determined with an uncertainty, since an expected value is calculated on the basis of a large number of samples, which is calculated with a standard deviation. In future experiments, it will be investigated how large the standard deviation of the individual parameters can be so that the smallest changes in the transfer functions can be reliably determined and are not lost in the standard deviation of the fitting factors ϑ_i .

5 CONCLUSION AND OUTLOOK

In this paper, a measurement system typically used in practice was tested under laboratory conditions with respect to its temperature dependence and its time-dependence. A method for the temperature compensation of LTSs was presented and furthermore a BMU was applied, with which a temperature compensation function can run semi-automatically over time.

It is shown that the generation of the temperature-dependent transfer function must first be applied on the structure to be monitored in order to perform reliable temperature compensation.

Furthermore, the application of a BMU with TMCMC algorithm shows a reliable fitting of the temperature-dependent transfer function over time. Thus, this procedure providing the interpreting engineer with a helpful tool for semi-automated temperature compensation in the presence of time-variant behavior of the measurement system.

Future studies will address the time variance of the measurement system in more detail. In addition, the uncertainty of the BMU must be taken into account when calculating the transfer function so that marginal change in the measurement system and at the structure can be reliably captured. This is the only way to reliably assess structures using monitoring systems over several years.

ACKNOWLEDGEMENT

This research was funded by the German Research Foundation (DFG), as part of the Collaborative Research Centre 1463 (SFB 1463) “Integrated Design and Operation Methodology for Offshore Megastructures” (subproject C01, project number 434502799).

REFERENCES

- Bartels, J.-H., Gebauer, D., & Marx, S. 2023. Einflüsse auf die Messunsicherheit von SHM-Systemen und deren Kompensation am Beispiel von Laser-Distanzmessungen. *Bautechnik*. Advance online publication. <https://doi.org/10.1002/bate.202200102>
- Berns, K.; Köpper, A.; Schürmann, B. 2019. Technische Grundlagen Eingebetteter Systeme. Elektronik, Systemtheorie, Komponenten und Analyse. Wiesbaden: Heidelberg.
- Ching, J. & Chen, Y.-C. 2007. Transitional Markov chain Monte Carlo method for Bayesian model updating, model class selection, and model averaging. In *Journal of Engineering Mechanics* (7), pp. 816–832.
- Dorsch, Rainer G.; Häusler, Gerd; Herrmann, Jürgen M. 1994. Laser triangulation: fundamental uncertainty in distance measurement. In *Appl. Opt.* (33), pp. 1306–1314.
- Farrar, C. R.; Worden, K. 2007. An introduction to structural health monitoring. In *Phil. Trans. R. Soc. A.* (365), pp. 303–315.
- Hübler, C.; Hofmeister, B.; Wernitz, S.; Rolfes, R. 2022. Validierung von daten- und modellbasierten Methoden zur Schadenslokalisierung. In *Bautechnik* (99), pp. 433–440.
- Li, S.; Caracoglia, L. 2019. Surrogate Model Monte Carlo simulation for stochastic flutter analysis of wind turbine blades. In *Journal of Wind Engineering and Industrial Aerodynamics* (188), pp. 43–60.
- Löffler-Mang, M. 2012. Triangulation. In *Optische Sensorik*. Vieweg + Teubner Verlag.
- Lye, A.; Cicirello, A.; Patelli, E. 2021. Sampling methods for solving Bayesian model updating problems: A tutorial. In *Mechanical Systems and Signal Processing* (159), pp. 1–43.
- Mares, C.; Dratz, B.; Mottershead, J. E.; Friswell, M. I. 2006. Model updating using Bayesian estimation. In *International Conference on Noise and Vibration Engineering, Katholieke Universiteit Leuven*, pp. 18–20.
- Murakami, F. 1994. Accuracy assessment of a laser triangulation sensor. In *Conference Proceedings. 10th Anniversary. IMTC/94. Advanced Technologies in I & M. 1994 IEEE Instrumentation and Measurement Technology Conference*, pp. 802–805.
- Wedel, F.; Marx, S. 2022. Application of Machine Learning Methods on Real Bridge Monitoring Data. In *Engineering Structures* (250), pp. 1–47.
- Worden, K.; Tomlinson, G. R. 2019. *Nonlinearity in Structural Dynamics*: CRC Press.
- Worden, K.; Farrar, C. R.; Manson, G.; Park, G. 2007. The fundamental axioms of structural health monitoring. In *Proc. R. Soc. A.* (463), pp. 1639–1664.